

Study of the kinetics and mechanism of the hydrogen evolution reaction on $CeMe_2Ge_2$ electrodes ($Me = Fe, Co, Ni$)

A.B. SHEIN^{1*}, V.I. KICHIGIN¹, M. KONYK², L. ROMAČKA², Yu. STADNYK²

¹Department of Physical Chemistry, Perm State University,
Bukireva St. 15, 614000 Perm, Russia

²Department of Inorganic Chemistry, Ivan Franko National University of Lviv,
Kyryla i Mefodiya St. 6, 79005 Lviv, Ukraine

*Corresponding author. E-mail: ashein@psu.ru

Received August 21, 2013; accepted December 25, 2013; available on-line August 30, 2014

The hydrogen evolution reaction on the $CeMe_2Ge_2$ ($Me = Fe, Co, Ni$) germanides in x M $H_2SO_4 + (0.5-x)$ M Na_2SO_4 ($x = 0.05-0.5$) solutions has been studied using polarization and impedance measurements. The conclusion has been made that hydrogen evolution on the investigated materials occurs by the Volmer-Tafel mechanism for a logarithmic isotherm of adsorption of atomic hydrogen.

Intermetallic compound / Hydrogen evolution reaction / Hydrogen adsorption / Acidic solution / Impedance

Introduction

Intermetallic cerium compounds are interesting subjects in the search for valence changes, or mixed valence states that generate phenomena such as Kondo lattice or heavy fermion behavior. The $CeMe_2Ge_2$ ($Me = Fe, Co, Ni$) ternary compounds belong to a long series of RMe_2Ge_2 intermetallics where R = rare earths; $Me = Mn, Fe, Co, Ni, Cu, Ag, Au, Ru, Pd$, or Pt , which crystallize with tetragonal structures of the $CeAl_2Ga_2$ -type (space group $I4/mmm$, ordered variant of the $BaAl_4$ -type) [1-4].

Intermetallic compounds (IMC) belong to a number of electrode materials considered to be promising as hydrogen evolution reaction (HER) catalysts [5-8]. In this group of materials, binary systems with a particular element ratio ($LaNi_5$, $MoNi_3$, $MoFe_3$, WFe_3 , etc.) may demonstrate high activity in HER. Some IMC have the ability to absorb large amounts of hydrogen, from the gas phase (at moderate pressures and temperatures) or during cathodic polarization in electrolytes [9,10], reversibly. This has attracted interest to these compounds as hydrogen storage materials and to the study of their cathodic behavior.

A significant number of studies have been carried out on partially substituted IMC, for example on $LaNi_{5-x}Me_x$, where Me is a metal. In [11] it was shown that partial replacement of Ni by Ge reduced the hydrogen capacity, but accelerated the hydrogen absorption and desorption: for $x \geq 0.3$ the exchange current on an alloy with Ge was higher than on the binary alloy and continued to increase with increasing values of x .

Below, the results of a study of the cathodic behavior of compounds $CeMe_2Ge_2$ ($Me = Fe, Co, Ni$) in acidic sulfate solutions are presented. As far as we know, HER and hydrogen absorption reaction (HAR) on these IMC in electrolytes have not yet been investigated.

Experimental

The samples were prepared by arc melting the constituent elements (Ce, purity 99.9 wt.%; iron, purity 99.99 wt.%; cobalt, purity 99.98 wt.%; nickel, purity 99.98 wt.%; germanium, purity 99.999 wt.%) under high-purity Ti-gettered argon atmosphere with a non-consumable tungsten electrode on a water-cooled copper hearth. The overall weight losses were generally less than 1 wt.%. The alloys were annealed at 870 K for 720 h in evacuated quartz ampoules, and finally quenched in cold water.

Phase analysis was performed and the crystallographic parameters determined using X-ray powder patterns recorded with a DRON-4.0 powder diffractometer (Fe $K\alpha$ radiation). XRPD data for structure refinements were collected in the transmission mode on a STOE STADI P diffractometer (linear PSD detector, $2\theta/\omega$ -scan; Cu $K\alpha_1$ radiation, curved germanium (111) monochromator). The lattice parameters were determined using the CSD program package [12]. Rietveld refinements were performed using the WinPLOTR program package [13].

Electrochemical measurements were made in x M H_2SO_4 + $(0.5-x)$ M Na_2SO_4 ($x = 0.05, 0.15$ and 0.5) solutions prepared from high-purity chemicals and deionised water (Milli Q), at temperatures of 22-24°C. The solutions were de-aerated by hydrogen (of 99.999% purity). An electrochemical cell with separate cathodic and anodic compartments was used. Before the experiment the electrode surfaces were successively stripped with sandpapers of grits 1000 and 2000, degreased with ethanol and washed with a working solution. Polarization and impedance measurements were carried out using a 1287 Electrochemical Interface device coupled with a 1255 Frequency Response Analyzer (Solartron Analytical). The frequency range used in the impedance measurements was from 10'000 to 0.01 Hz (10 points per decade). The amplitude of the alternating signal was 10 mV. The current was stabilized before measuring at each potential. For measuring and processing the impedance data, CorrWare2, ZPlot2 and ZView2 programs (Scribner Associates, Inc.) were used. The values of the potential (E) are given in the normal hydrogen electrode (nhe) scale.

Results and discussion

The X-ray powder diffraction measurements confirmed that the $CeMe_2Ge_2$ ($Me = Fe, Co, Ni$) compounds under investigation crystallize with tetragonal structures in space group $I4/mmm$. The lattice parameters derived from the X-ray patterns are: $a = 0.40695(5)$ nm, $c = 1.04984(2)$ nm for Fe; $a = 0.4064(3)$ nm, $c = 1.0147(2)$ nm for Co; $a = 0.41572(2)$ nm, $c = 0.98613(7)$ nm for Ni. No foreign Bragg peaks were observed, hence confirming the single-phase character of the samples. A complete crystal structure investigation of $CeCo_2Ge_2$ was reported in [14], whereas for the $CeMe_2Ge_2$ compounds with Fe and Ni only the lattice parameters have been determined. During the present work, detailed crystal structure refinements were performed for $CeFe_2Ge_2$ and $CeNi_2Ge_2$; the refined atomic parameters are given in Table 1 ($R_B = 0.030$, $R_p = 0.020$, $R_{wp} = 0.025$ for Fe, $R_B = 0.081$, $R_p = 0.031$, $R_{wp} = 0.039$ for Ni). As example, the

observed, calculated and difference X-ray patterns for the $CeFe_2Ge_2$ compound are shown in Fig. 1.

The polarization curves in sulfate solution have two Tafel plots (Fig. 2). In 0.5 M H_2SO_4 the Tafel slope b_1 of the first plot is 0.067 V, whereas the Tafel slope b_2 of the second plot is 0.170-0.190 V. The order of the HER with respect to the hydrogen ions – $(\partial \lg i / \partial pH)_E$ for the $CeNi_2Ge_2$ electrode is equal to 1.0 for the plot with lower slope and ~ 0.45 for the plot with higher slope.

The point break on the polarization curves moves to higher current densities (i) in the order $CeNi_2Ge_2 < CeCo_2Ge_2 \approx CeFe_2Ge_2$.

A slope of the polarization curve equal to ~ 0.06 V in semi-logarithmic coordinates can have several explanations. Assuming a Langmuir isotherm of hydrogen adsorption, $b \approx 0.06$ V can be observed for a barrierless discharge of hydrogen ions [15], or at the rate-limiting step of surface diffusion of adsorbed hydrogen atoms H_{ads} [16]. Slow, barrierless discharge is in this case unlikely, because such a mechanism is possible for metals with relatively low hydrogen adsorption energy E_{M-H} , but our investigated IMC contain cerium and iron group metals that possess high energy of hydrogen adsorption [17]. The presence of a surface diffusion step can be considered as probable, since different atoms are present in the investigated materials and the discharge of H_3O^+ ions and the combination of adsorbed hydrogen atoms into a molecule can occur at different sites (centers) of the metal surface. According to [18], when the rate-determining step is surface diffusion, then the Tafel slope is 0.079 V, but not 0.06 V, and $(\partial \lg i / \partial \lg C_{H^+})_\eta = 0.25$. The last parameter is not consistent with the experimentally observed value (for $CeNi_2Ge_2$).

Since the investigated IMC are characterized by considerable hydrogen adsorption energy, surface coverage by H_{ads} can also be significant. Therefore it is reasonable to compare the experimental results with theoretical ones, obtained with the assumption of a logarithmic isotherm of hydrogen adsorption, which can take place at medium coverage θ of the electrode surface by hydrogen ($0.2 < \theta < 0.8$). Theoretical values of some coefficients on the logarithmic isotherm of hydrogen adsorption, obtained by the analysis of the work in [19], are given in Table 2.

Table 1 Atomic positional and isotropic displacement parameters for the $CeFe_2Ge_2$ and $CeNi_2Ge_2$ compounds.

Site	Me	Wyckoff position	x	y	z	$B_{iso} \cdot 10^2$ (nm ²)
Ce	Fe	2a	0	0	0	0.45(5)
	Ni					0.48(3)
Me	Fe	4d	0	1/2	1/4	1.00(7)
	Ni					0.63(4)
Ge	Fe	4e	0	0	0.3745(1)	0.88(7)
	Ni				0.3826(6)	1.05(3)

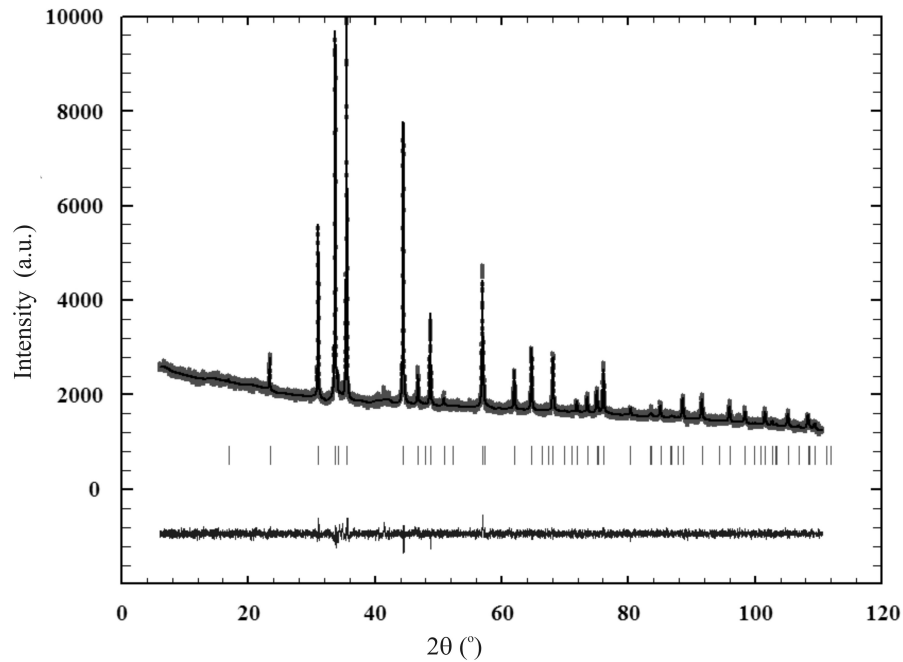


Fig. 1 Observed, calculated and difference X-ray patterns of the $CeFe_2Ge_2$ compound.

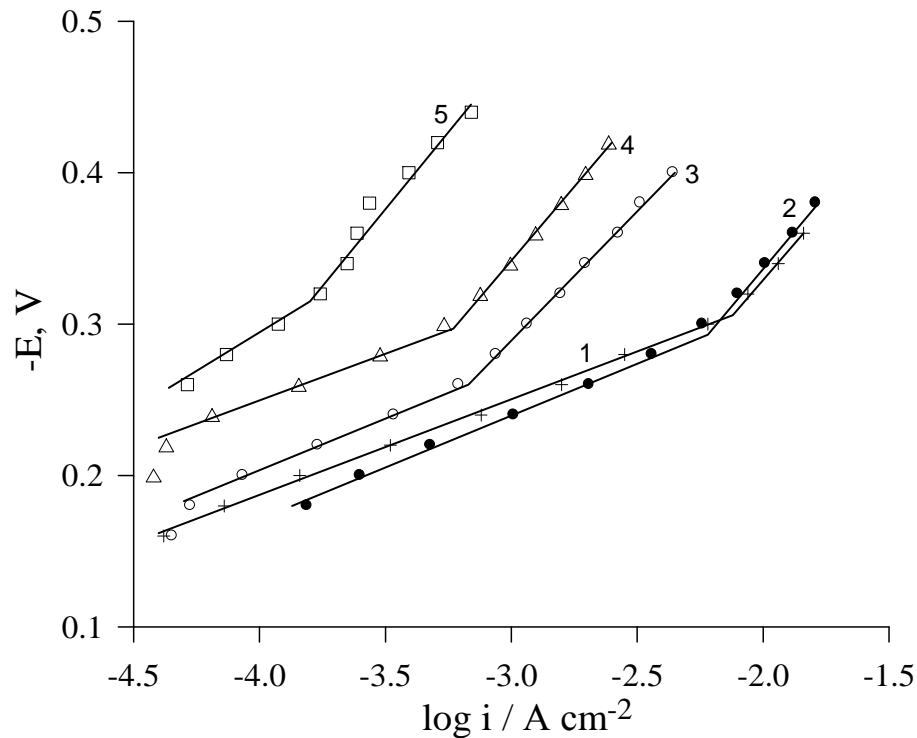


Fig. 2 Polarization curves in x M H_2SO_4 + $(0.5-x)$ M Na_2SO_4 solutions. 1 – $CeFe_2Ge_2$; 2 – $CeCo_2Ge_2$; 3-5 – $CeNi_2Ge_2$. For curves 1-3: $x = 0.5$, for 4: $x = 0.15$, for 5: $x = 0.05$.

In this table α and γ are transfer coefficients for the Volmer and Heyrovsky steps, respectively, β is the ratio of the change in the activation energy of hydrogen desorption with coverage to the change in the heat of adsorption with coverage.

The experimental polarization curves with two Tafel plots and the $(\partial \lg i / \partial pH)_E$ values for the $CeNi_2Ge_2$ electrode can be explained within the framework of the Volmer-Tafel mechanism for activated adsorption of H_2 . The best agreement with the experiment is obtained for $\alpha = 0.62$, $\beta = 0.47$.

Table 2 Parameters of the HER for a logarithmic isotherm of hydrogen adsorption [19].

HER mechanism		Parameter		
		$-\frac{dE}{d \lg i}$	$\frac{dE}{d \lg C_{H^+}}$	$\left(\frac{\partial \lg i}{\partial \lg C_{H^+}}\right)_E$
Volmer-Tafel	Quasi-equilibrium discharge, non-activated adsorption	$\frac{2.3RT}{F}$	$\frac{2.3RT}{F}$	1
	Quasi-equilibrium discharge, activated adsorption	$\frac{2.3RT}{2\beta F}$	$\frac{2.3RT}{F}$	2β
	Both stages irreversible, non-activated adsorption	$\frac{2.3RT}{F} \left(\frac{2+\alpha}{2\alpha}\right)$	$\frac{2.3RT}{\alpha F}$	$\frac{2}{2+\alpha}$
	Both stages irreversible, activated adsorption	$\frac{2.3RT}{F} \left(\frac{\alpha+2\beta}{2\alpha\beta}\right)$	$\frac{2.3RT}{\alpha F}$	$\frac{2\beta}{\alpha+2\beta}$
Volmer-Heyrovsky	Quasi-equilibrium discharge	$\frac{2.3RT}{2\gamma F}$	$\frac{2.3RT}{F} \left(\frac{1+\gamma}{2\gamma}\right)$	$1+\gamma$
	Both stages irreversible	$\frac{2.3RT}{F} \cdot \frac{\alpha+\gamma}{2\alpha\gamma}$	$\frac{2.3RT}{F} \left(\frac{\alpha+\gamma}{2\alpha\gamma}\right)$	1

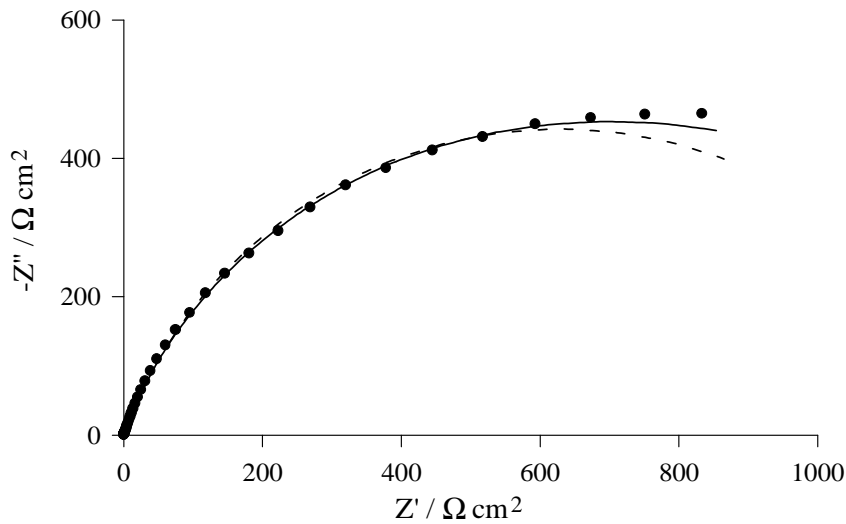


Fig. 3 Nyquist diagrams of a $CeFe_2Ge_2$ electrode in 0.5 M H_2SO_4 at $E = -0.14$ V. Symbols are experimental data, the dashed line is the result of calculations according to the equivalent circuit A (Fig. 5,A), the solid line is the result of calculations according to the equivalent circuit B (Fig. 5,B).

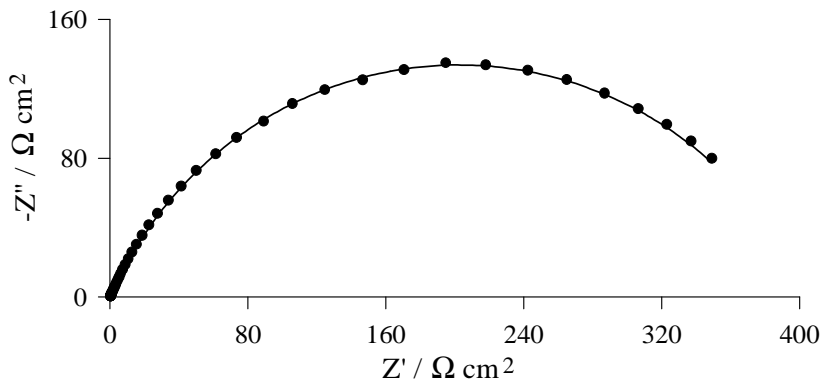


Fig. 4 Nyquist diagram of a $CeFe_2Ge_2$ electrode in 0.5 M H_2SO_4 at $E = -0.18$ V. Symbols are experimental data, the solid line is the result of calculations according to the equivalent circuit A (Fig. 5,A).

Impedance spectra in Nyquist coordinates are presented in Figs. 3 and 4. In order to describe the experimental impedance spectra, two equivalent electric circuits were used (Fig. 5). Circuit A is a model of a two-step process of HER type with intermediate adsorption [20,21]; circuit B is a model of HER taking into consideration the hydrogen absorption reaction (HAR) that occurs with diffusion limitations [21,22]. In circuit B an absorption resistance R_{ab} , connected in series with a hydrogen diffusion impedance Z_d , is not used, since according to most researchers [23], the hydrogen transfer from the adsorbed to absorbed state is very fast. The physical meaning of the Faraday impedance parameters in these models is discussed in [20-22]. In both equivalent circuits, instead of an electric double layer capacity, we have used a constant phase element CPE [24], which models the double layer charging process on a heterogeneous electrode surface more precisely. The form of equivalent circuit for HER does not depend on the type of isotherm of atomic hydrogen adsorption.

At moderate cathodic polarizations the equivalent circuit B describes the experimental impedance data much better (Fig. 3), but the simpler circuit A can be used at more negative potentials for a quantitative description of the experimental impedance spectra

(Fig. 4). The hydrogen absorption reaction is not associated with any charge transfer and its kinetics do not directly depend on the electrode potential, therefore the contribution of HAR to the electrode immittance decreases with increasing cathodic polarization [25].

Dependencies of the parameters of the equivalent circuit A on the potential of the CeFe_2Ge_2 electrode are shown in Fig. 6. Within a certain range of potential the resistance R_1 is almost constant, but increases for low cathodic polarizations. On going from 0.5 M H_2SO_4 to 0.15 M H_2SO_4 + 0.35 M Na_2SO_4 , the resistance R_1 increases on the average by a factor 1.6-1.7, but with further decrease of the concentration of hydrogen ions up to 0.05 M, the resistance R_1 returns to the values observed for 0.5 M H_2SO_4 . During processing of the data with the help of the ZView program, we noted that, although at some electrode potentials $R_1 \ll R_2$, the uncertainty on the R_1 values does not exceed 15%, and at those potentials at which a distinction between R_1 and R_2 is not so significant, the uncertainty on R_1 decreases to 2-3%.

In all the studied solutions the resistance R_2 varies exponentially with the electrode potential and increases with decreasing hydrogen ion concentration. The slope of the $\log R_2$ - E lines is 15.0-15.2 V^{-1} , which is slightly lower than $F/(2.303RT)$.

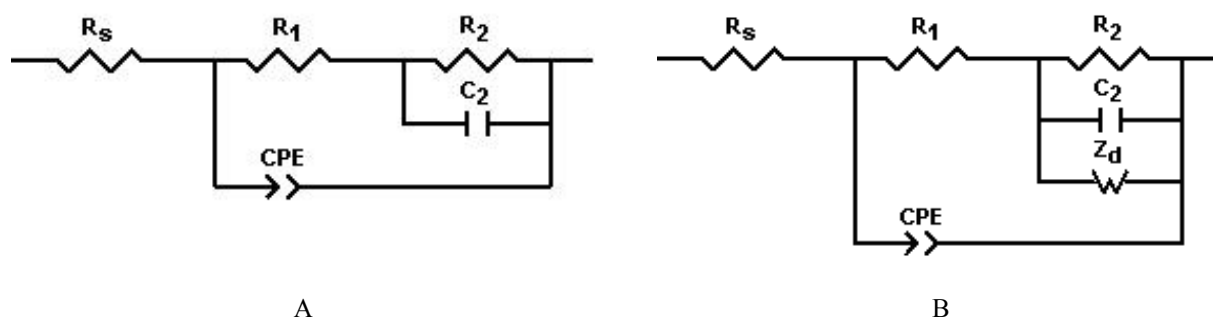


Fig. 5 Equivalent electric circuits: A – for HER process; B – for HER + HAR process. R_s is the solution resistance.

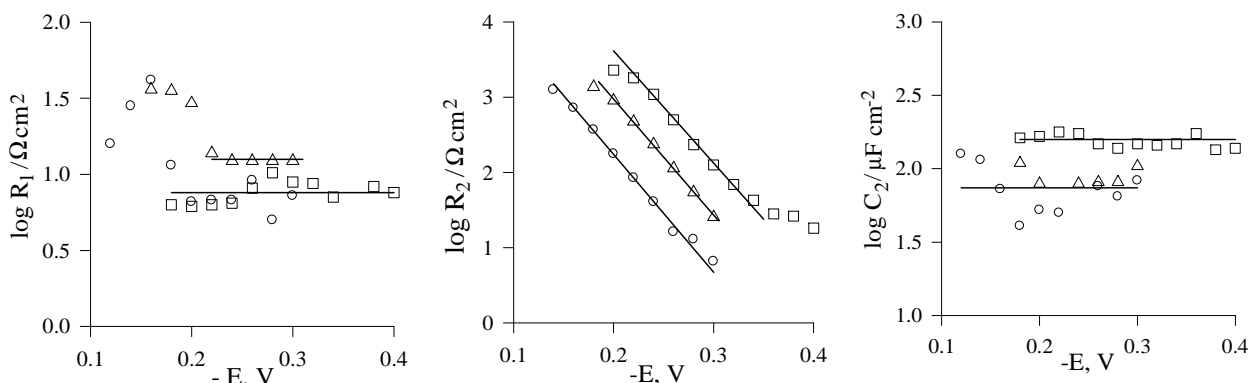


Fig. 6 Dependencies of the parameters of the equivalent circuit A (Fig. 5,A) on the potential of a CeFe_2Ge_2 electrode for different concentrations of hydrogen ions: (o) 0.5 M H_2SO_4 ; (Δ) 0.15 M H_2SO_4 + 0.35 M Na_2SO_4 ; (\square) 0.05 M H_2SO_4 + 0.45 M Na_2SO_4 .

The results (Fig. 6) are, to a first approximation, consistent with a HER mechanism, the assumption of which was made on the basis of polarization measurements, namely a Volmer-Tafel mechanism at a logarithmic Temkin isotherm. The kinetic equations for the Volmer and Tafel steps can in this case be written in the form [19,26]:

$$i_V = k_V a_{H^+} \exp(-\alpha f \theta) \exp(-\alpha FE / RT) - k_{-V} \exp[(1-\alpha) f \theta] \exp[(1-\alpha) FE / RT] \quad (1)$$

$$i_T = k_T \exp(2\beta f \theta) \quad (2)$$

where k_V and k_{-V} are rate constants of the Volmer reaction in forward and reverse directions, k_T the rate constant of the Tafel reaction, a_{H^+} the activity of the hydrogen ion near the electrode surface, f a factor of surface inhomogeneity, which determines the dependence of the free energy of hydrogen adsorption on the coverage: $\Delta G_{ads} = \Delta G_{ads, \theta=0} + fRT\theta$. The coefficients α and β were introduced earlier. Equations (1) and (2) are valid for medium coverages ($0.2 < \theta < 0.8$), where changes in θ and $(1-\theta)$ can be neglected, as compared with changes in $\exp(-\alpha f \theta)$ and other exponents with θ .

Assuming quasi-equilibrium at the Volmer step, we obtain the following expression for the coverage:

$$\theta = \frac{1}{f} \left[\ln \left(\frac{k_V a_{H^+}}{k_{-V}} \right) - \frac{FE}{RT} \right] \quad (3)$$

In accordance with the general expressions for equivalent circuit A parameters [20], for the Volmer-Tafel route it is possible to obtain the following equations:

$$R_1 = \frac{RT}{F^2} \frac{1}{(k_V a_{H^+})^{1-\alpha} (k_{-V})^\alpha} \quad (4)$$

$$R_2 = \frac{RT}{F^2} \frac{\exp\left(\frac{2\beta FE}{RT}\right)}{2\beta (k_V a_{H^+})^{2\beta} (k_{-V})^{-2\beta} k_T} \quad (5)$$

$$C_2 = \frac{q_1 F}{fRT} \quad (6)$$

where q_1 is the charge required for the formation of a H_{ads} monolayer. From equations (4)-(6) it follows that, in the range of potentials in which the assumption of quasi-equilibrium at the Volmer step is valid, the resistance R_1 and capacity C_2 do not depend on E . The resistance R_2 decreases with increasing cathodic polarization, and the slope of the linear dependence of $\log R_2$ on E is equal to $2\beta F / (2.303RT)$. The capacity C_2 does not depend on the concentration of H⁺ ions, and the resistances R_1 and R_2 decrease with increasing H⁺

ion concentration. Moreover, the dependence of R_2 on a_{H^+} is stronger than for R_1 .

The results, shown in Fig. 6 for CeFe₂Ge₂, approximately correspond to equations (4)-(6). Indeed, in a certain range of E the parameters R_1 and C_2 do not depend on E . The slope of the $\log R_2$ - E lines that is equal to 15.0-15.2 V⁻¹, corresponds to a theoretical slope at $\beta = 0.44$ -0.45. The resistance R_1 depends less on the hydrogen ion concentration than R_2 , while the dependence of R_1 on a_{H^+} does not fully correspond to equation (4). The capacity C_2 for the CeFe₂Ge₂ electrode is on the average equal to 150 μF/cm². Assuming $q_1 = 200$ μC/cm², to obtain values of C_2 in accordance with (6) it is necessary to accept that f takes very high values (about 50). In this case the charge q_1 is probably significantly less than 200 μC/cm², which may explain the observed values of C_2 without the assumption of too high f values. The possibility of deviations of q_1 from ~200 μC/cm² towards lower values has been observed, for example, for Pt electrodes [27]. The capacity C_2 slightly depends on a_{H^+} (Fig. 6); this does not follow from equation (6), but the dependence may be due to the influence of a_{H^+} on the values of f and/or q_1 .

In the case of irreversible stages, it follows from the kinetic equations (1) and (2):

$$\theta = \frac{1}{f(\alpha + 2\beta)} \left[\ln \left(\frac{k_V a_{H^+}}{k_T} \right) - \frac{\alpha FE}{RT} \right] \quad (7)$$

In this case, from the general expressions for the parameters of the equivalent circuit A given in [20], we can obtain the following equations:

$$R_1 = \frac{RT}{F^2} \frac{\exp\left(\frac{2\alpha\beta FE}{\alpha + 2\beta RT}\right)}{\alpha (k_V a_{H^+})^{2\beta/(\alpha+2\beta)} (k_T)^{\alpha/(\alpha+2\beta)}} \quad (8)$$

$$R_2 = \frac{RT}{F^2} \frac{\exp\left(\frac{2\alpha\beta FE}{\alpha + 2\beta RT}\right)}{2\beta (k_V a_{H^+})^{2\beta/(\alpha+2\beta)} (k_T)^{\alpha/(\alpha+2\beta)}} \quad (9)$$

and equation (6) remains for the capacity C_2 . Thus, at sufficiently low potentials the resistance R_1 starts to change with E and the slope of the $\log R_2$ - E straight line decreases (3 times at $\alpha = \beta = 0.5$), as compared with the slope in the area of quasi-equilibrium of the Volmer reaction. A decrease of the slope of the dependence of $\log R_2$ on E is observed in the experiment, for example, for the CeFe₂Ge₂ electrode in a 0.05 M H₂SO₄ + 0.45 M Na₂SO₄ solution, beginning from $E \approx -0.34$ V (Fig. 6), however, the decrease of the slope is not accompanied by a reduction of R_1 .

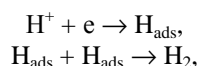
The decrease of R_1 at low potentials is observed also for the CeCo₂Ge₂ electrode (Fig. 7), but here the potentials at which the $\log R_1$ - E and $\log R_2$ - E

dependencies break do not coincide. The potential of break in the $\log R_2$ - E dependence is close to the position of the point of break on the polarization curve.

The character of the dependencies of the parameters of the equivalent circuit A on the potential of the CeNi_2Ge_2 electrode is qualitatively similar to the character of the corresponding dependencies for the CeFe_2Ge_2 electrode (Fig. 6), but the values of R_1 for CeNi_2Ge_2 are noticeably lower.

Conclusion

The obtained polarization and impedance characteristics of CeMe_2Ge_2 electrodes ($Me = \text{Fe}, \text{Co}, \text{Ni}$) in acidic sulfate solutions are mostly consistent with the Volmer-Tafel mechanism, *i.e.* a sequence of reactions



assuming a logarithmic Temkin isotherm for the adsorption of hydrogen atoms on the electrode surface. However, we can notice a discrepancy between the theoretical predictions for this mechanism and the experimental data – the difference between the potentials at which break points appear on the experimental dependencies of $\log R_1$ and $\log R_2$ on E . In order to clarify the reasons of this discrepancy, further research and development of more accurate models for the electrode process are needed.

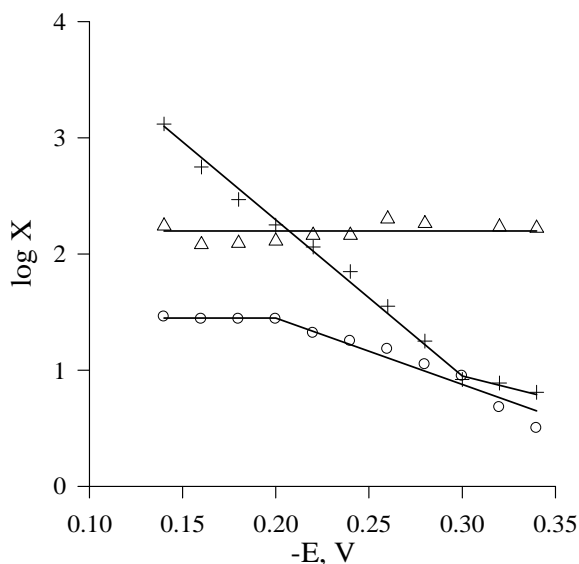


Fig. 7 Dependencies of the parameters of the equivalent circuit A (Fig. 5,A) on the potential of a CeCo_2Ge_2 electrode in a 0.15 M H_2SO_4 + 0.35 M Na_2SO_4 solution. $X = R_1$ (o); R_2 (+); C_2 (Δ). The values of R_1 and R_2 are in $\text{Ohm}\cdot\text{cm}^2$, C_2 in $\mu\text{F}\cdot\text{cm}^2$.

References

- [1] A.V. Morozkin, Y.D. Seropegin, A.V. Gribanov, J.M. Barakatova, *J. Alloys Compd.* 256 (1997) 175-191.
- [2] A.P. Murani, A. Loidl, K. Knorr, G. Knopp, A. Krimmel, R. Caspary, A. Böhm, G. Sparrn, C. Geibel, F. Steglich, *Phys. Rev. B: Condens. Matter* 46 (1992) 9341-9351.
- [3] J.J. Bara, H.U. Hryniewicz, A. Milos, A. Szytula, *J. Less-Common Met.* 161 (1990) 185-192.
- [4] A. Szytula, I. Szott, *Solid State Commun.* 40 (1981) 199-202.
- [5] M.M. Jakšić, C.M. Lacnjevac, B.N. Grgur, N.V. Krstajić, *J. New Mater. Electrochem. Syst.* 3 (2000) 131-144.
- [6] S.H. Jordanov, P. Paunović, O. Popovski, A. Dimitrov, D. Slavkov, *Bull. Chem. Technol. Maced.* 23 (2004) 101-112.
- [7] F. Rosalbino, G. Borzone, E. Angelini, R. Raggio, *Electrochim. Acta* 48 (2003) 3939-3944.
- [8] F. Rosalbino, D. Maccio, A. Saccone, E. Angelini, S. Delfino, *J. Alloys Compd.* 431 (2007) 256-261.
- [9] O.A. Petrii, S.Ya. Vasina, I.I. Korobov, *Usp. Khim.* 65 (1996) 195-210.
- [10] J. Kleperis, G. Wójcik, A. Czerwinski, J. Skowronski, M. Kopczyk, M. Beltowska-Brzezinska, *Solid State Electrochem.* 5 (2001) 229-249.
- [11] C. Witham, A. Hightower, B. Fultz, B.V. Ratnakumar, R.C. Bowman, *J. Electrochem. Soc.* 144 (1997) 3758-3764.
- [12] L.G. Akselrud, Yu.N. Grin, P.Yu. Zavalii, V.K. Pecharsky, *Coll. Abstr. 12 Eur. Crystallogr. Meet.*, Nauka, Moscow, 1989, Vol. 3, p. 155.
- [13] J. Rodriguez-Carvajal. *FULLPROF: A Program for Rietveld Refinement and Pattern Matching Analysis*, version 3.5d; Laboratoire Léon Brillouin (CEA-CNRS), Saclay, France, 1998.
- [14] R. Rawat, V.G. Sathe, *J. Phys.: Condens. Matter* 17 (2005) 313-322.
- [15] L.I. Krishtalik, *Electrochim. Acta* 13 (1968) 1045.
- [16] M. Fleischmann, M. Grenness, *J. Chem. Soc., Faraday Trans. 1* 68 (1972) 3205-3215.
- [17] L.I. Krishtalik, In: P. Delahay (Ed.) *Advances in Electrochemistry and Electrochemical Engineering*, Intersci. Publ., New York, 1970, Vol. 7, pp. 283-340.
- [18] A.V. Vvedensky, I.A. Gutorov, N.B. Morozova, *Condens. Matter Interphases* 12(3) (2010) 288-300.
- [19] J.G.N. Thomas, *Trans. Faraday Soc.* 57 (1961) 1603-1611.
- [20] D.A. Harrington, B.E. Conway, *Electrochim. Acta* 32 (1987) 1703-1712

- [21] A. Lasia, in: B.E. Conway and R. White (eds.), *Modern Aspects of Electrochemistry*, Kluwer Academic/Plenum Publishers, New York, 2002, Vol. 35, pp. 1-49.
- [22] C. Lim, S.-I. Pyun, *Electrochim. Acta* 38 (1993) 2645-2652.
- [23] C. Gabrielli, P.P. Grand, A. Lasia, H. Perrot, *J. Electrochem. Soc.* 151 (2004) A1943-A1949.
- [24] G.J. Brug, A.L.G. van den Eeden, M. Sluyters-Rehbach, J.H. Sluyters, *J. Electroanal. Chem.* 176 (1984) 275-295.
- [25] E.R. Gonzalez, M.J. de Giz, *Chem. Ind.* 54 (2000) 123-132.
- [26] E.J. Kelly, H.R. Bronstein, *J. Electrochem. Soc.* 131 (1984) 2232-2238.
- [27] L. Bai, D.A. Harrington, B.E. Conway, *Electrochim. Acta* 32 (1987) 1713-1731.